ACS SyntheticBiology

pubs.acs.org/synthbio

Research Article

Introducing an Artificial Deazaflavin Cofactor in *Escherichia coli* and *Saccharomyces cerevisiae*

Misun Lee,[§] Jeroen Drenth,[§] Milos Trajkovic, René M. de Jong, and Marco W. Fraaije*

Cite This: *ACS Synth. Biol.* 2022, 11, 938−952

Read Online

ACCESS | Metrics & More | Article Recommendations | Supporting Information

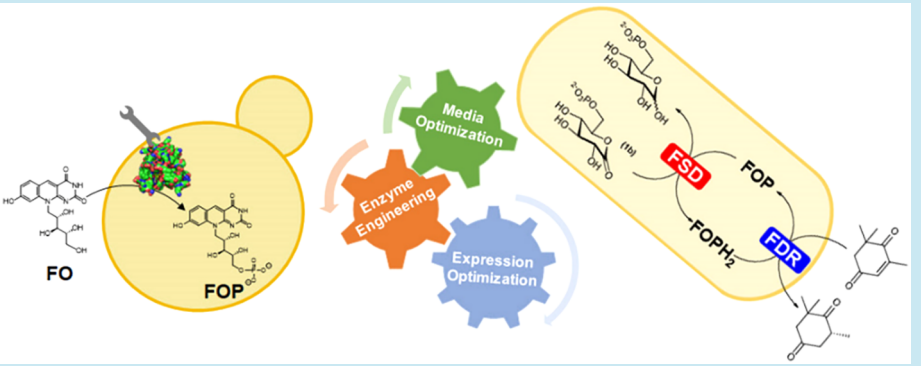

ABSTRACT: Deazaflavin-dependent whole-cell conversions in well-studied and industrially relevant microorganisms such as *Escherichia coli* and *Saccharomyces cerevisiae* have high potential for the biocatalytic production of valuable compounds. The artificial deazaflavin FOP (FO-5′-phosphate) can functionally substitute the natural deazaflavin F_{420} and can be synthesized in fewer steps, offering a solution to the limited availability of the latter due to its complex (bio)synthesis. Herein we set out to produce FOP in vivo as a scalable FOP production method and as a means for FOP-mediated whole-cell conversions. Heterologous expression of the riboflavin kinase from *Schizosaccharomyces pombe* enabled in vivo phosphorylation of FO, which was supplied by either organic synthesis ex vivo, or by a coexpressed FO synthase in vivo, producing FOP in *E. coli* as well as in *S. cerevisiae*. Through combined approaches of enzyme engineering as well as optimization of expression systems and growth media, we further improved the in vivo FOP production in both organisms. The improved FOP production yield in *E. coli* is comparable to the F_{420} yield of native F_{420}-producing organisms such as *Mycobacterium smegmatis*, but the former can be achieved in a significantly shorter time frame. Our *E. coli* expression system has an estimated production rate of 0.078 μmol L^{-1} h^{-1} and results in an intracellular FOP concentration of about 40 μM, which is high enough to support catalysis. In fact, we demonstrate the successful FOP-mediated whole-cell conversion of ketoisophorone using *E. coli* cells. In *S. cerevisiae*, in vivo FOP production by *Sp*RFK using supplied FO was improved through media optimization and enzyme engineering. Through structure-guided enzyme engineering, a *Sp*RFK variant with 7-fold increased catalytic efficiency compared to the wild type was discovered. By using this variant in optimized media conditions, FOP production yield in *S. cerevisiae* was 20-fold increased compared to the very low initial yield of 0.24 ± 0.04 nmol per g dry biomass. The results show that bacterial and eukaryotic hosts can be engineered to produce the functional deazaflavin cofactor mimic FOP.

KEYWORDS: *deazaflavin, F_{420}, artificial cofactor, whole-cell conversion, cofactor biosynthesis*

Asymmetric hydrogenations are important for the synthesis of high value compounds, such as pharmaceuticals. Some of these can be synthesized under mild conditions by enzymatic reductions of imines, ketones, and activated C=C bonds, with high enantiomeric access.[1] Cofactor F_{420}-dependent oxidoreductases show a high potential as biocatalysts for these kinds of reactions.[2,3] The low redox potential of −360 mV,[4] when compared to other coenzymes like FAD (−219 mV),[5] FMN (−205 mV),[6] and NAD(P)$^+$ (−320 mV), makes F_{420} an excellent reducing agent. Furthermore, this 7,8-didemethyl-8-hydroxy-5-deazaflavin (Figure 1) is an obligate two-electron carrier, like NAD(P)H, which prevents potential radical side reactions and ensures a high tolerance to molecular oxygen.[7,8] Whereas the flavin (FAD/FMN) and nicotinamide (NAD$^+$/NADP$^+$) cofactors are ubiquitous in all existing life forms, the deazaflavin cofactor F_{420} is mainly found in Actinobacteria and methanogenic archaeal species.[9,10]

Received: November 1, 2021
Published: January 19, 2022

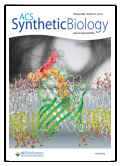

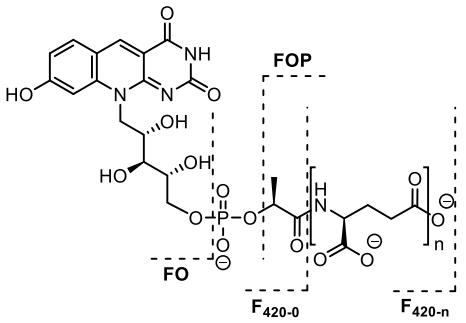

Figure 1. Structure of F_{420} and its precursors FO and F_{420-0}, as well as the artificial cofactor analogue FO-5′-phosphate, FOP.

Despite the potential use of the high reduction power and various reaction scopes of F_{420} for interesting industrial applications,[2] its low availability hampers further exploration and exploitation of the cofactor and its respective deazaflavin-dependent enzymes. Although F_{420} can be purified from methanogens and Actinobacteria such as *M. smegmatis*, extraction from these organisms only yields several micromoles per liter of culture.[10,11] Furthermore, using these organisms in industrial settings is not favorable due to the slow growth and potential hazards related to the cultivating condition and pathogenicity.[10] Therefore, F_{420} production in more commonly used microorganisms by genetic and metabolic engineering is of great interest. Recent studies show that heterologous expression of the F_{420}-biosynthetic pathway in *E. coli* can produce the cofactor as well, albeit with lower yields than that produced naturally in *M. smegmatis* (~27 nmol L^{-1} of culture in *E. coli*, compared to 1.43 μmol L^{-1} in *M. smegmatis*).[10,12,13] The heterologous production yield of the cofactor can be improved through optimizing growth conditions as it was demonstrated in a follow-up study.[14]

As an elegant alternative to F_{420}, we previously showed that the chemoenzymatically synthesized artificial biomimetic deazaflavin FOP (FO-5′-phosphate, Figure 1) is also accepted by a range of F_{420}-dependent enzymes and can be produced in comparatively higher amounts.[15] The low water solubility of the chemically synthesized precursor FO, as well as the stability of the employed kinase, make upscaling for industrial applications still challenging. Furthermore, the relatively costly ATP used for in vitro phosphorylation is also an upscaling obstacle. In vivo FOP production, however, could overcome the aforementioned complications, as a cost efficient, green, and scalable alternative. The two-step biosynthesis of FOP, using a FO synthase and an engineered riboflavin kinase, could also be a more viable alternative to the multistep biosynthesis of F_{420}. Producing FOP in commonly used microorganisms such as *E. coli* or yeast can help advance F_{420}-related research. These organisms are easy to handle, and well-established genetic tools are available for enzyme and strain engineering. And using strains such as *S. cerevisiae*, which is recognized as a GRAS organism ("generally recognized as safe"), is an advantage for industrial production of pharma- or food-related compounds.

In this study, we explore FOP production in both *E. coli* and *S. cerevisiae* in view of future applications in large scale production of the artificial F_{420} biomimetic for in vitro purposes, as well as whole-cell FOP-mediated conversions. These whole-cell approaches could have several advantages, such as (1) no need for enzyme purification, (2) no need for in vitro FOP synthesis, (3) easy catalyst−product separation, (4) low cost, and (5) no need for additional cofactors and sacrificial electron donors, as these are already present in the cell.

In F_{420}-producing organisms the catalytic core, FO, is synthesized by radical SAM-dependent reactions that are catalyzed by either a single bifunctional enzyme (FbiC) or two enzymes (CofG and CofH).[9,16,17] The starting materials for FO biosynthesis, tyrosine and 5-amino-6-ribitylamino-2,4[1H,3H]-pyrimidinedione, are ubiquitous metabolites.[18] FO synthesis could therefore also be performed in *E. coli* and *S. cerevisiae* by heterologous expression of a FO synthase (FbiC or a combination of CofG and CofH). Phosphorylating the 5′-position of the D-ribitol moiety of FO would then yield the unnatural cofactor FOP. Herein we show the successful de novo biosynthesis of FOP in *E. coli* by coexpressing FO-synthase and a riboflavin kinase from *Schizosaccharomyces pombe* (*Sp*RFK) with a two-plasmid system (Scheme 1). *Sp*RFK showed higher activity than the previously used engineered kinase from *Corynebacterium ammoniagenes* (*Ca*RFK).[15] Furthermore, unlike *Ca*RFK which is a bifunctional riboflavin kinase/FMN adenylyltransferase, *Sp*RFK is a monofunctional riboflavin kinase so that the truncation, which may decrease enzyme stability, is not required. The FOP production in *E. coli* was further optimized by structure-guided RFK engineering, as well as varying the FO synthases, *E. coli* expression strains, expression temperatures, expression vectors, and growth media. Gratifyingly, this resulted in FOP yields similar to F_{420} yields in *M. smegmatis*.

A hybrid synthesis approach was used to produce FOP in *S. cerevisiae* by using heterologously expressed *Sp*RFK and FO supplemented to the media. We focused on the optimization of in vivo phosphorylation of FO in *S. cerevisiae* due to the low FOP yield. We first analyzed the effect of media composition on FOP production and discovered that supplementary riboflavin and

Scheme 1. De Novo Biosynthesis of FOP in *E. coli*[a]

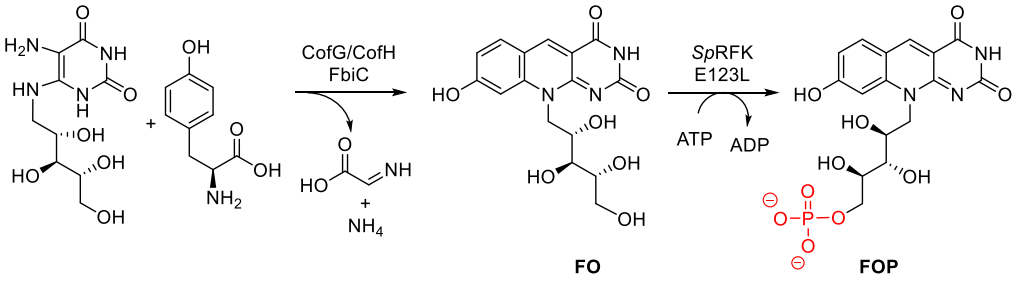

[a]The FO synthase synthesizes FO using tyrosine and 5-amino-6-ribitylamino-2,4[1H,3H]-pyrimidinedione. Subsequent 5′-phosporylation by an engineered riboflavin kinase from *S. pombe* yields FOP (FO-5′-phosphate).

https://doi.org/10.1021/acssynbio.1c00552
ACS Synth. Biol. 2022, 11, 938−952

amino acids as well as FO concentration in media affect the final FOP yield significantly. Engineering of *Sp*RFK was also employed to increase the FOP yield. By screening 90 in silico designed variants based on the in vivo FOP yield, we identified a variant showing more than a 2-fold higher yield than the wild type kinase. By using the optimized FO kinase and growth media optimization, we achieved a significantly improved FOP production in *S. cerevisiae*.

By demonstrating the in vivo FOP production in *E. coli* and *S. cerevisiae* and several approaches to improve the yield, this study facilitates further development of both bacteria- and yeast-based whole-cell deazaflavin-mediated reductions and/or production of deazaflavin cofactors.

MATERIALS AND METHODS

Strains and Cloning. The bacterial expression and cloning strains *Escherichia coli* NEB 10-beta, BL21 (DE3), and C41 (DE3) were obtained from New England Biolabs (NEB, Ipswich, MA, U.S.A.). *S. cerevisiae* strain CEN. PK2−1C was purchased from Euroscarf. All genes used for FOP production and whole-cell FOP-mediated conversion in *E. coli* were codon-optimized and synthesized by GenScript Biotech, with flanking 5′-NcoI/3′-*Hin*dIII or 5′-NdeI/3′-PacI restriction sites for cloning into multiple cloning site 1 (MCS1) or 2 (MCS2) of the used Duet vectors, respectively. Genes were cloned into the Duet-vectors by restriction/ligation, using standard protocols. For in vivo FO phosphorylation experiments in *E. coli*, the codon-optimized *Sp*RFK was cloned into a pBAD vector. The mutant E123L was constructed on this vector using a standard site-directed mutagenesis method. For in vitro characterization of *Sp*RFK, a codon-optimized gene was cloned into a pBAD vector with N-terminal 6xHis-tag using the Golden Gate assembly method.[19] These vector constructs were transformed into *E. coli* NEB 10-beta for vector amplification and storage.

All plasmids used for *S. cerevisiae* work were assembled using a modular vector cloning kit (MoClo-YTK, Addgene) following the protocol of Lee et al.[20] For FOP production in *S. cerevisiae*, a codon-optimized *Sp*RFK gene with 5′- and 3′-flanking regions containing BasI and BsmBI restriction sites was purchased from Twistbioscience and assembled into a 2 μ-based *E. coli*−yeast shuttle vector (pTEF-*Sp*RFK). The transcription of the *Sp*RFK gene in *S. cerevisiae* was regulated by the pTEF1 promoter and a tTDH1 terminator. The URA3 gene was used as an auxotrophic marker. The sequences of the optimized genes can be found in Table S1. Table S2 shows all the constructs from this study.

Purification of *Sp*RFK. For in vitro characterization, *Sp*RFK was expressed in *E. coli* NEB 10-beta. The expression was induced by adding 0.2% (v/v) L-arabinose to the pBAD-N-6 × His-*Sp*RFK harboring *E. coli* culture in Terrific Broth (TB) containing 50 mg/L ampicillin. After the growth at 37 °C for 16 h, the culture was harvested. The N-terminal 6xHis-tagged *Sp*RFK was purified using metal affinity chromatography (Ni-NTA) by the means of gravity flow. The buffers used for the purification are as follows: A, 50 mM KPi, pH 7.4; B, buffer A + DNase (20 μg/mL) + 1 mM $MgCl_2$ + 1 mM PMSF; C, buffer A + 15 mM imidazole; D, buffer A + 500 mM imidazole. The harvested cells were washed with buffer A and resuspended in buffer B subsequently. The cells were disrupted by sonication (Sonics Vibra-Cell VCX 130 sonicator, cycle of 2 s on and 4 s off for 4 min at 70% amplitude) and the cell debris was removed by centrifugation for 40 min at 31 000*g*, 4 °C. The supernatant was applied to the Ni-NTA resin that was pre-equilibrated with buffer A. The column was washed with 10 column volume of buffer A and 20 column volume of buffer C, subsequently. *Sp*RFK was eluted with three column volumes of buffer D. The eluent was desalted using EconoPac 10-DG desalting column (Bio-Rad) pre-equilibrated with buffer A.

FO Synthesis. 7,8-Didemethyl-8-hydroxy-5-deazariboflavin (FO) was chemically synthesized as described previously by Drenth et al.[15]

In Vitro Activity of Purified *Sp*RFK. One milliliter reaction mixtures containing 50 μM FO, 0.5 mM ATP, 2 mM Mg^{2+} and 1 μM *Sp*RFK were incubated at 30°, pH 7.0 (50 mM HEPES) for 1 h. The reaction was stopped by heating the sample at 95 °C for 10 min and the precipitants were removed by centrifugation at 17 000*g* for 10 min. The reaction was analyzed by HPLC and LC-MS.

Steady-State Kinetic Measurements. To determine the kinetic parameters, wild-type *Sp*RFK and variants were expressed in *E. coli* and purified as described above. The reactions were performed at 30 °C, pH 7.0 (50 mM KPi) in a total volume of 1 mL. The reaction mixtures contained different concentrations of FO, ranging from 5 to 400 μM, 0.5 mM ATP, 2 mM Mg^{2+}, and 0.1 μM *Sp*RFK. 150 μL of the mixtures were collected at 5, 10, 15, 20, and 25 min and the reactions were stopped by heating the samples at 95 °C for 5 min. After centrifugation to remove aggregates, the samples were analyzed by HPLC. The concentration of the produced FOP at each time point was calculated using the purified FOP calibration curve and then used to calculate k_{obs} (s^{-1}) at each FO concentration. The calculated k_{obs} values were plotted against the FO concentration and were fitted to the Michaelis−Menten model, using GraphPad Prism 6 to determine the kinetic parameters.

FMN Inhibition. One milliliter reaction mixtures containing 50 μM or 200 μM FO, 0−10 μM FMN, 0.5 mM ATP, 2 mM Mg^{2+}, and 1 μM *Sp*RFK were incubated at 30°, pH 7.0 (50 mM HEPES). After 20 min, the reactions were stopped by heating at 95 °C for 10 min. The samples were cleaned up by centrifugation at 17 000*g* for 10 min and the FOP conversion was analyzed by HPLC

Enzyme Expression and FO/FOP Production in *E. coli* Strains. pETDuet_CofG/H, pETDuet_*Sc*FbiC, and pETDuet_*Ms*FbiC were transformed into *E. coli* BL21 (DE3) or C41 (DE3) for FO synthase expression and FO production screening. Either pCDFDuet_*Sp*RFK E123L or pRSFDuet_*Sp*RFK E123L was cotransformed into *E. coli* BL21 (DE3) or C41 (DE3) with either pETDuet_CofG/H, pETDuet_*Sc*FbiC, or pETDuet_*Ms*FbiC for in vivo FOP production. Single transformation colonies were picked and grown overnight at 37 °C, 135 rpm, in 5 mL terrific broth (TB) with the appropriate antibiotic(s). The overnight cultures were diluted 1:100 in 50 mL fresh TB, LB or M9 medium, supplemented with either 1% glucose (w/v) or 1% glycerol (w/v), in 250 mL Erlenmeyer flasks, with the same antibiotic(s). The cultures were incubated at 37 °C, 135 rpm for 3 h, after which the cultures were induced with 1 mM isopropyl β-D-1-thiogalactopyranoside (IPTG). The cultures were further incubated at 24 or 37 °C, 135 rpm, for 12 to 20 h.

FO and FOP Isolation from *E. coli* and Analysis. The cultures described above were harvested by centrifugation (4000*g*, 20 min, 4 °C, Beckman-Coulter centrifuge) and the pellets were resuspended in 5 mL 50 mM Tris-HCl, pH 8 containing 1 $\mu g\ mL^{-1}$ DNase, 1 $\mu g\ mL^{-1}$ lysozyme and 0.1 mM phenylmethylsulfonyl fluoride (PMSF). The cells were lysed by sonication, using a Sonics Vibra-Cell VCX 130 sonicator with a 3 mm stepped microtip (5s on, 5 s off, 70% amplitude, 10 min)

https://doi.org/10.1021/acssynbio.1c00552
ACS Synth. Biol. 2022, 11, 938−952

and the extracts were cleared by centrifugation (8000*g*, 45 min, 4 °C). The amount of in vivo produced FO and FOP was quantified by HPLC analysis. FO that may leak out of the cells to the media[10] was not included in the measurement. Samples were prepared in the following way: 300 μL formic acid and 1 mL of cell-free extracts (CFE) were mixed and incubated on ice for 5 min. Then, 200 μL 1.6 mM NaOH was added and spun down at 8000*g*, 4 °C, for 15 min. Ten μL supernatant was used for analysis. For further calculations the following assumptions were made: 1 $OD_{600} \triangleq 0.396$ gDCW L^{-1}, 1 $OD_{600} \triangleq 7.8 \times 10^8$ cells mL^{-1}, and the *E. coli* cell volume is 4.4×10^{-15} L.[21,22]

Whole-Cell Conversion Using FOP-Producing *E. coli*. The plasmid vectors pETDuet_*Ms*FbiC, pCDFDuet_*Sp*RFK E123L, and pCOLADuet_FSD/FDR were cotransformed into *E. coli* C41 (DE3). Cultures were grown and expressed in TB as described for FOP production. After harvesting, cell pellets were resuspended in M9 medium, containing 1% glycerol (w/v) and 1 mM IPTG. Reactions were initiated by adding cells to a final OD_{600} of 6.25 in M9 medium with 1% glycerol, 1 mM IPTG, 7.5 mM ketoisophorone, and 2% DMSO (v/v), in a total volume of 5 mL. Reaction mixtures were incubated at 37 °C, 250 rpm in 24-deep well plates. Reactions were quenched by adding three parts acetonitrile to 1 part of medium, after spinning down the cells. This mixture was incubated on ice for 5 min and then spun down at 8000*g* in a table top centrifuge at 4 °C, for 15 min. Afterward, 10 μL supernatant was used for HPLC analysis. The depletion of substrate was analyzed at 240 nm, using an isocratic mobile phase of 60:40 acetonitrile:water on an Alltech Alltime HP C18 5 μ, 250 mm column. The formation of the correct product was analyzed by GC-MS and chiral GC, as described previously.[23]

Media Used for *S. cerevisiae*. Two types of media were used for the growth of *S. cerevisiae* carrying pTEF-*Sp*RFK plasmids and for in vivo FOP production. SC medium used here is a synthetic defined media lacking uracil and containing 2% glucose. It is composed of 6.9 g/L yeast nitrogen base without amino acids (YNB) and 0.77 g/L complete supplement mixtures without uracil, both of which were purchased from Formedium. Another media used is YND medium which contains YNB (6.9 g/L) and 2% glucose. YND is supplemented with 76 mg/L each L-tryptophan and L-histidine as well as 340 mg/L L-leucine. Yeast nitrogen base without amino acids and riboflavin (Formedium) was used for testing the effect of riboflavin on FOP production. For in vivo FOP production, 200 μM (unless otherwise stated) FO was added to the medium before autoclave sterilization.

In Vivo FOP Production in *S. cerevisiae* and FOP Isolation. For in vivo FOP production in *S. cerevisiae*, overnight-grown (at 30 °C) preinoculum of the yeast cells expressing *Sp*RFK were diluted to OD_{600} 0.4 in 25 mL of either SC or YND medium with or without riboflavin (SC-RF and YND-RF, respectively), containing 200 μM FO. The preinoculum was grown in the respective medium without FO. After growing for 24 h at 30 °C in FO containing medium, cells were harvested by centrifugation (3000*g* for 10 min) and washed with 50 mL Milli-Q water. For isolation of intracellular FOP, cells were resuspended in 2 mL 70% boiling ethanol, incubated for 5 min at 95 °C, and spun down for 10 min at 17 000*g*. The cell extract solutions were collected and the procedure was repeated once more. The collected extract solutions were lyophilized and resuspended in 250 μL of Milli-Q. After cleaning up by centrifugation the samples were analyzed by HPLC. To estimate the FOP yield per g dry cell weight (DCW), the correlation between the measured OD_{600} and measured cell dry weight was determined. *S. cerevisiae* grown until the late exponential phase was diluted to OD_{600} values of 3−8 in 1 mL, in triplicates. The samples were dried by lyophilization and the measured dry cell weights were plotted against the OD_{600}/mL.

HPLC Analysis of FO and FOP. Samples were separated on a Phenomenex Gemini C18 (4.6 × 250 mm, 5 μm) column. A linear gradient of 50 mM ammonium acetate pH 6.0 with 5% acetonitrile (buffer A) and 100% acetonitrile (buffer B) was applied at a flow rate of 1 mL/min: t = 0 min/100:0 (A:B), t = 16 min/80:20 (A:B), t = 19 min/5:95 (A:B), t = 22 min/5:95 (A:B), t = 26 min/95:05 (A:B), t = 28 min/100:0 (A:B). The separation was monitored in time with UV absorbance at 262 nm and fluorescence (ex: 400 nm and em: 470 nm). FOP concentration was calculated based on the peak area calibration curve which was made with the purified FOP. Retention times for FOP and FO were 11 and 12.7 min, respectively.

FOP Purification. Enzymatically synthesized FOP using *Sp*RFK was purified on a C18 column (FlashPure 24 mL, Buchi). The quenched and filtered reaction solution was loaded onto the column which was pre-equilibrated sequentially with methanol and Milli-Q. After washing with 50 mL Milli-Q water, FOP was eluted with 5% methanol and lyophilized for further use.

LC-MS Analysis of FOP from in Vitro Conversion. To verify the FOP produced by the *Sp*RFK reaction, the mass of the reaction product was analyzed using a UPLC-MS system (Acquity-TQD, Waters). The reaction sample was separated on a ACQUITY UPLC HSS T3 column (1.8 μm, 2.1 × 150 mm, Waters) using a gradient between solvent A (0.1% formic acid in water) and solvent B (0.1% formic acid in acetonitrile) at a flow rate of 0.31 mL/min: t = 0 min/100:0 (A:B), t = 5 min/75:25 (A:B), t = 6.12 min/5:95 (A:B), t = 7.14 min/5:95 (A:B), t = 8.16 min/75:25 (A:B), t = 9.18 min/100:0 (A:B). Electrospray ionization (ESI) in negative ion mode was used for mass detection.

LC-MS Verification for the Presence of FOP in *E. coli* Cell-Free Extract. The presence of FOP in cell-free extracts was determined by UPLC/ESI-QTOF-MS. *E. coli* cell-free extract (CFE) samples were processed in the same way as for HPLC (mentioned above), a 3 μL sample was injected onto a Acquity UPLC BEH C18 (50 × 2.1 mm, 1.7 μm, Waters) column. The mobile phase consisted of solvent A (0.1% formic acid in water) and solvent B (0.1% formic acid in acetonitrile). Compounds were separated by the following program at a flow rate of 0.3 mL/min: linear gradient from 99 to 5% A (v/v) in 10 min, kept at 5% A for 0.5 min, returning to 99% A in 1 min, re-equilibration to 99% A in 3 min. The separation was measured by absorbance at 400 nm. The mass spectrometer detected negative ions over the mass/charge range (m/z) 100−600.

***Sp*RFK Library Design and Construction.** The previously solved X-ray structure of *Sp*RFK (PDB: 1N07)[24] was used as the initial structure for Rosetta calculations[25] of FOP binding. The structure was processed in Schrodinger and a ligand FMN molecule in the structure was turned into FOP manually. The resulting protein-FOP complex was used for flexible backbone design using the CoupledMoves algorithm available in Rosetta 3.5.[26] 10 Amino acids (Ile43, Thr45, Val64, Val79, Ser81, Arg121, Glu123, Leu132, Ile136, and Asp139) surrounding the FOP molecule were allowed to be mutated to all possible amino acids in 20 parallel runs (nstruct = 20 flag) of 10 000 Monte Carlo sampling steps (ntrials = 10000 flag), to ensure full

https://doi.org/10.1021/acssynbio.1c00552
ACS Synth. Biol. 2022, 11, 938−952

coverage of possible mutations compatible with FOP in the active site. The FOP molecule was allowed to participate in the design via rigid body moves without constraints to further improve acceptance rate of FOP-compatible mutations. Other flags for the CoupledMoves command were kept at their default values, except for the ligand_weight, which was set to 2.0, thus ensuring increased weight of ligand-protein interactions in the Rosetta energy calculations. After removing redundant designs from the 20 parallel runs, 90 amino acid variants were selected based on the most commonly occurring mutations in the 400 designs with the lowest Rosetta energy and manual inspection of the top design structures produced by the algorithm. The *Sp*RFK mutant library was constructed based on the Golden Gate assembly method.[19] The gene fragments containing the mutations were designed in two parts based on the mutated residues: the N-terminal part of the gene covering the mutations on residues Thr45 and Val79 or Val64 and Ser81 and the C-terminal part of the gene covering the mutations on Glu123 and Leu132. The required 25 gene fragments with flanking regions containing BsaI and BsmBI restriction sites were purchased from Integrated DNA Technologies, Inc. Prior to the library assembly, each fragment was cloned into an entry vector containing the ColE1 origin of replication and chloramphenicol resistance marker via a BsmBI Golden Gate reaction. The resulting plasmids were transformed in *E. coli*, amplified and purified. These plasmids were used for sequencing of the fragments and further library assembly. After verification of the fragment sequences, each entry vector containing the N-terminal part fragment and the C-terminal part fragment were combined to generate all desired 90 variants and assembled into a 2 μ-based expression vector (pTEF-*Sp*RFK) using BsaI Golden Gate assembly. The selection of correct mutant constructs was done through *E. coli* transformation, colony picking, amplification, and sequencing. The correct variants were transformed in *S. cerevisiae* using an optimized lithium acetate-based method[27] and the transformants were plated on a solid SC medium.

Library Screening by Measuring the *S. cerevisiae* in Vivo FOP Formation. *S. cerevisiae* cells containing *Sp*RFK variants were grown overnight at 30 °C in 5 mL SC medium in 24-well plates. The preinoculum was then diluted in 2 × 5 mL SC medium containing 200 μM FO in 24 well plates and cultivated at 30 °C. After 24 h, the cultures were harvested and washed with Milli-Q water by centrifugation at 3200*g* for 15 min. To isolate FOP, cells were resuspended in 500 μL 70% boiling ethanol, incubated for 5 min at 95 °C, and spun down for 10 min at 13 000*g*. The cell extract solutions were collected and the procedure was repeated once more. The collected extract solutions were lyophilized and resuspended in 100 μL of Milli-Q water. After cleaning up by centrifugation, the samples were analyzed by the aforementioned HPLC method.

RESULTS

In Vitro Conversion of FO. Owing to the similar structures of riboflavin and FO, riboflavin kinase is a good target enzyme for enzymatic FOP production. Previously, it was shown that an engineered riboflavin kinase from *C. ammoniagenes* (*Ca*RFK) could accept FO as a substrate and produce FOP.[15] Three hydrophobic residues near the 7-methyl and 8-methyl groups of riboflavin were mutated to two more polar residues and one longer apolar residue (F21H/Y_F85H_A66I/V) so that the 7-demethyl and 8-hydroxyl groups of FO could be accommodated. Comparing the X-ray crystal structures of *Ca*RFK and *Sp*RFK, we realized that the mutations at two of the residues already exist in *Sp*RFK; His98 and Val79 correspond to Phe85 and Ala66 in *Ca*RFK, respectively (Figure 2). This led us to explore the possibility of using *Sp*RFK for more efficient FOP production.

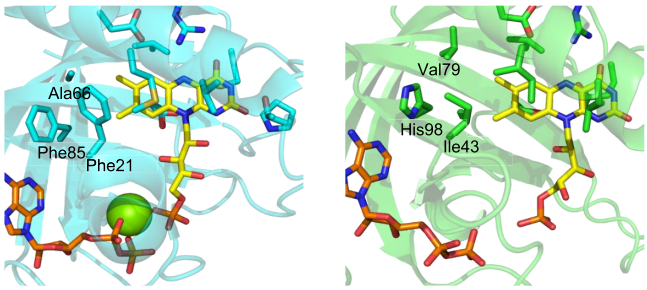

Figure 2. Riboflavin binding site structures of *Ca*RFK (left, PDB: 5A89)[28] and *Sp*RFK (right, PDB: 1N07).[24] Amino acid residues that are within 6 Å radius of the isoalloxazine ring of FMN are shown in sticks. FMN and ADP molecules are depicted as a yellow and orange sticks, respectively. Mg^{2+} ion is shown in a green sphere.

For testing the substrate acceptance of the wild-type *Sp*RFK, the enzyme was expressed in *E. coli* NEB 10-beta and purified. The expression of the *E. coli*-codon optimized *Sp*RFK gene in this strain yielded a good amount of soluble protein (50 mg/L culture) and the estimated size of the protein (~19 kDa) was confirmed by SDS-PAGE analysis. Surprisingly, after 1 h of incubation at 30 °C, the reaction containing 50 μM FO showed nearly full conversion, when analyzed by HPLC (Figure 3a). The formed product was analyzed by UPLC-MS and showed the corresponding mass of FOP (expected m/z 442.07, $[M-H]^-$) (Figure 3c). These data show that wild-type *Sp*RFK can catalyze the phosphorylation of the non-natural substrate FO with higher activity than the previously engineered *Ca*RFK variant.[15]

In vivo enzyme applications require the consideration of the possible interaction of the enzyme with any intracellular molecule. Because *Sp*RFK will likely perform its natural reaction of converting riboflavin in *S. cerevisiae*, we sought to test for any inhibition by either riboflavin or FMN in FO conversion. When the reaction was performed with an equimolar amount of riboflavin and FO, even after long incubation of 8 h, there was no conversion of FO whereas riboflavin was fully converted to FMN. This suggests that the presence of FMN might inhibit the phosphorylation of FO, which should be addressed when engineering the enzyme for in vivo conversion.

Structure-guided mutagenesis using the FMN-bound crystal structure of *Sp*RFK[24] was employed to further enhance the activity toward FOP. Mutant E123L was designed to better accommodate the C5 of FO in a more hydrophobic environment. The in vivo activity was measured by comparing the amount of FOP in cell-free extracts of *E. coli* NEB 10-beta, expressing the enzymes on a pBAD vector. HPLC analysis with UV and fluorescence detection was used to identify and quantify FOP in cell-free extracts. The measured FOP yield in cells expressing the mutant enzyme *Sp*RFK E123L was significantly higher than cells expressing wild-type enzyme, resulting in roughly double the amount of FOP (Figure 4a). Yet no significant differences in apparent expression levels (SDS-PAGE) and final cell densities (OD_{600}) were observed (Figure S1). Therefore, we concluded that the engineered kinase *Sp*RFK E123L is the best performing enzyme for in vivo FOP production in *E. coli*.

https://doi.org/10.1021/acssynbio.1c00552
ACS Synth. Biol. 2022, 11, 938−952

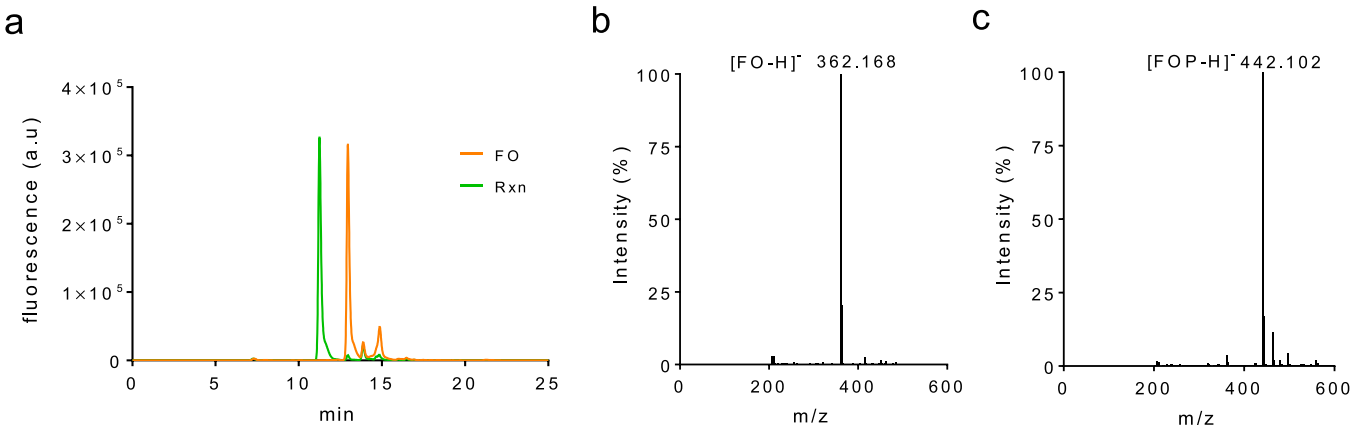

Figure 3. FO conversion by *Sp*RFK. (a) HPLC chromatogram of FO (orange line) and the formed product (green line). The retention times for FO and the reaction product were 12.9 and 11.2 min, respectively. (b) Mass verification of the substrate FO. (c) Mass verification of the reaction product FOP.

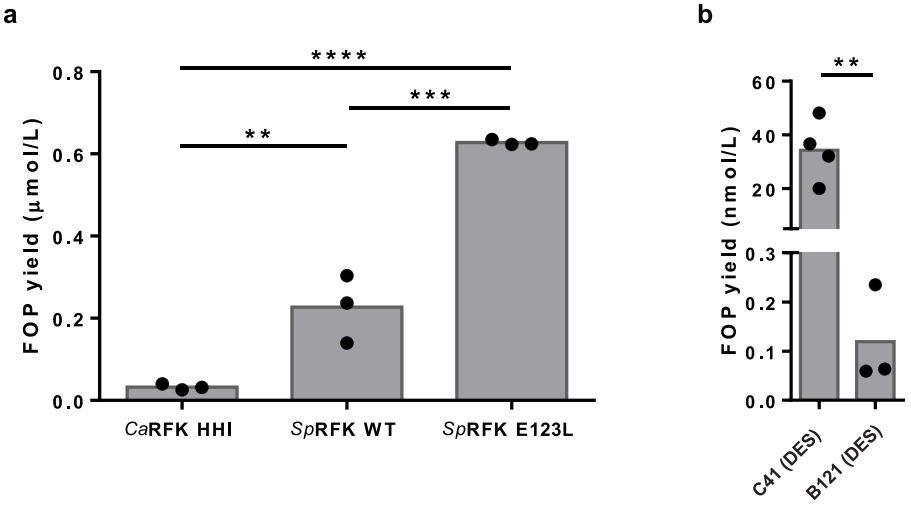

Figure 4. (a) FOP productivity in μmol FOP per liter of culture in *E. coli* NEB 10-beta cells expressing different riboflavin kinases from pBAD vectors. Bars represent mean values, which were calculated from 3 independent measurements, shown as dots. Data were analyzed by a one-way ANOVA, with Brown−Forsythe test, showing no significant difference in standard deviations. *$p \leq 0.05$; **$p \leq 0.01$; ***$p \leq 0.001$; ****$p \leq 0.0001$. (b) FOP yield from BL21(DE3) and C41 (DE3) cultures harboring pETDuet_*Sc*FbiC and pCDFDuet_*Sp*RFK E123L. FOP concentrations were measured in cell-free extracts of biological replicates by HPLC fluorescence detection. Bars represent average values, calculated from individual data points, shown as dots. An unpaired two-tailed *t* test with Welch's correction was applied to confirm a significant difference in FOP yields, with a *p*-value of 0.0099 (**).

In Vivo FOP Production: *E. coli* Expression Strain Selection. Three FO synthases were screened for their expression and in vivo activity in *E. coli* BL21 (DE23) and C41 (DE3). The FbiCs of *Streptomyces coelicolor* (*Sc*FbiC) and *M. smegmatis* (*Ms*FbiC), as well as the combination of CofG from *Methanocaldococcus jannaschii* (*Mj*CofG) and CofH from *Nostoc punctiforme* (*Np*CofH), were expressed on pETDuet-1 (~40 copies per cell). SDS-PAGE analysis showed the apparent expression of these FO synthases, and the expression level was higher in C41 (DE3) than BL21 (DE3) (Figure S2). FOP could be produced in both *E. coli* BL21 (DE3) and C41 (DE3) when pETDuet_*Sc*FbiC was coexpressed with pCDFDuet-1 (20−40 copies), harboring the *Sp*RFK E123L gene in MCS1. The FOP yield in *E. coli* C41 (DE3) cell-free extracts was significantly higher by more than 2 orders of magnitude, see Figure 4b, whereas no significant differences in final cell densities were observed. Therefore, C41 (DE3) was selected for further FOP production experiments.

HPLC was used for the detection of FOP (and FO) in cell-free extracts. In order to confirm that the peak with a retention time of 11 min was really due to the presence of FOP, LC-MS was performed on the samples. LC-MS indeed detected a compound with a corresponding *m*/*z* to FOP in *E. coli* C41 (DE3) expressing the two-plasmid system, which was absent in the CFE of wild type *E. coli* C41 (DE3), therefore confirming the presence of FOP with the two-plasmid system. See Supplementary Figure S4.

In Vivo FOP Production in C41 (DE3): Growth Temperature and Vector Construct Selection. The pETDuet vectors with the different FO synthase constructs were coexpressed in *E. coli* C41 (DE3) with pCDFDuet-1 (20−40 copies), harboring the *Sp*RFK E123L gene in MCS1. 50 mL cultures were grown in 250 mL Erlenmeyer flasks, induced with IPTG and grown at either 24 °C for 36 h or 37 °C for 16 h, after which the FOP concentration was measured. The FOP production was significantly larger at 37 °C for cultures expressing *Ms*FbiC and the CofG/CofH on pETDuet-1, with at least 10 times more FOP produced (Figure 5a). In order to see if we could increase the FOP production even more, *Sp*RFK E123L was also cloned into MCS1 of pRSFDuet-1 (>100

https://doi.org/10.1021/acssynbio.1c00552
ACS Synth. Biol. 2022, 11, 938−952

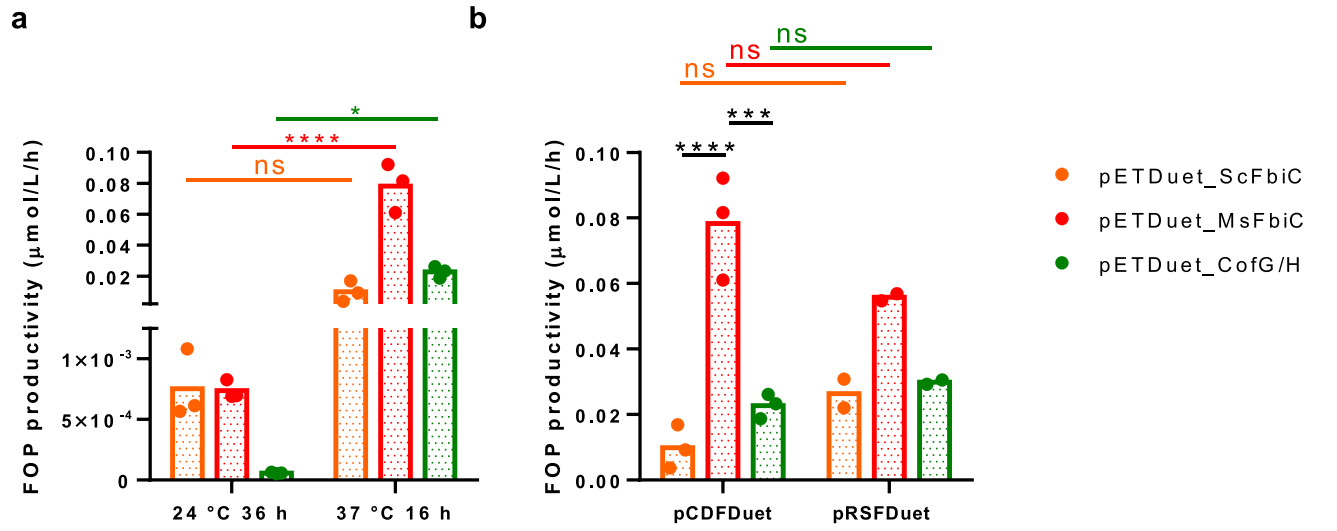

Figure 5. FOP productivity in μmol per liter of culture per hour of growth. The amount of FOP in cell-free extracts as measured by HPLC, using fluorescence detection. (a) FOP productivity by C41 (DE3) cells that express an FO synthase on pETDuet-1 and *Sp*RFK E123L on pCDFDuet-1 at 24 and 37 °C, after 36 and 16 h of growth, respectively. (b) FOP productivity by C41 (DE3) cells that express an FO synthase on pETDuet-1 and *Sp*RFK E123L on either pCDFDuet-1 or pRSFDuet-1. Bars represent mean values of individual data points that are depicted as dots. Data were analyzed by a two-way ANOVA. ns: not significant ($p > 0.05$); *$p \leq 0.05$; **$p \leq 0.01$; ***$p \leq 0.001$.

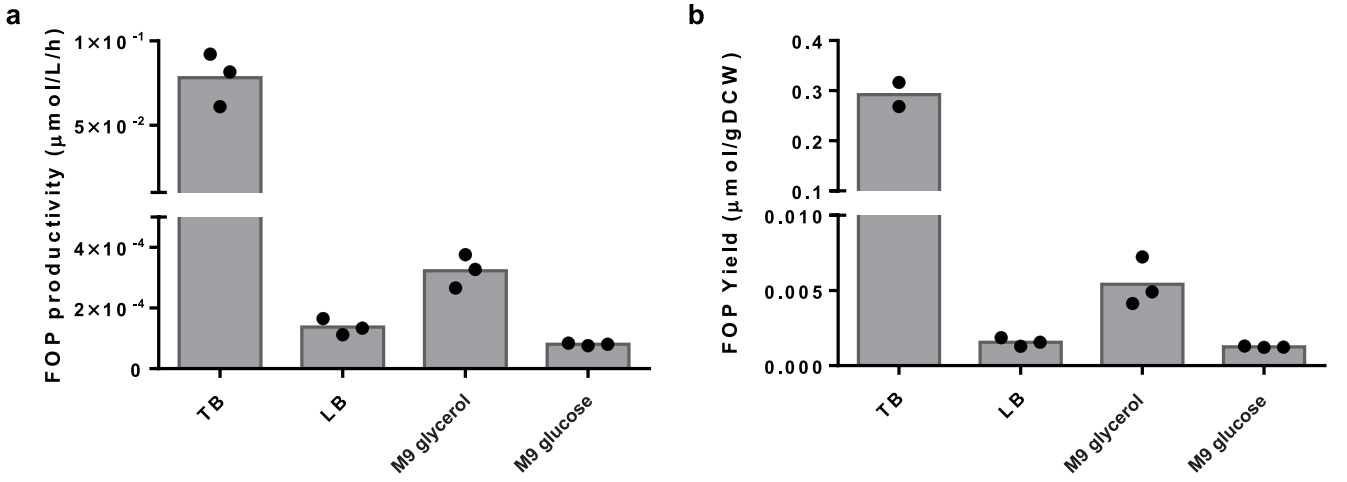

Figure 6. Effect of different commonly used growth media on FOP production by *E. coli* C41 (DE3) expressing *Ms*FbiC on pETDuet-1 and *Sp*RFK E123L on pCDFDuet-1. Bars represent mean values of individual data points that are depicted as dots.

copies). The cellular FOP concentration did not significantly increase or decrease as compared to using pCDFDuet-1 (Figure 5b). Also, the apparent protein concentration, as judged by SDS-PAGE of cell-free extracts, was comparable (Figure S3). Using pACYCDuet-1 (10−12 copies) for *Sp*RFK E123L expression, however, drastically decreased the FOP yield to negligible amounts.

The combination of pETDuet_*Ms*FbiC and either pCDFDuet-1 or pRSFDuet harboring *Sp*RFK E123L were the best performing FOP production systems, and resulted in yields of up to 1.24 μmol FOP per liter of culture (0.3 μmol gDCW^{-1}), within 16 h. This number is comparable to the natural F_{420} yield in *M. smegmatis*, which can reach 1.43 μmol L^{-1}.[10,13] The FOP production per unit of time, however, is greatly enhanced, as it takes 2−4 days of growth for *M. smegmatis* and other natural F_{420}-producing organisms before harvesting, whereas our system only takes 16 h, due to the fast growth of *E. coli*. This translates to a FOP productivity of 0.078 μmol L^{-1} h^{-1}.

FOP Production in C41 (DE3): Growth Media Selection. Terrific broth (TB) was used as the default medium in this study in order to determine the best combination of riboflavin kinase variant, plasmid constructs, temperature, and expression strain. Other commonly used media were then screened for their FOP production capacity. We selected the rich medium lysogeny broth (LB) and the defined M9 medium, with either 1% glucose (w/v) or 1% glycerol (w/v) as a carbon source. Using TB medium was the most beneficial, both in FOP production per culture volume per unit of time and in FOP production per gram dry cell weight (gDCW) (Figure 6). Supplementing TB with a saturating amount of 5 mM tyrosine (a precursor of FO) or 100 μM ammonium iron(II)sulfate, as previously was shown to benefit FO synthase expression by Graham et al.,[17] did not further increase the FOP yield.

Whole-Cell Conversion of Ketoisophorone. We estimated that intracellular FOP concentrations in *E. coli* C41 (DE3) can reach up to about 40 μM when these cells are coexpressing pETDuet_*Ms*FbiC and pCDFDuet_*Sp*RFK

https://doi.org/10.1021/acssynbio.1c00552
ACS Synth. Biol. 2022, 11, 938−952

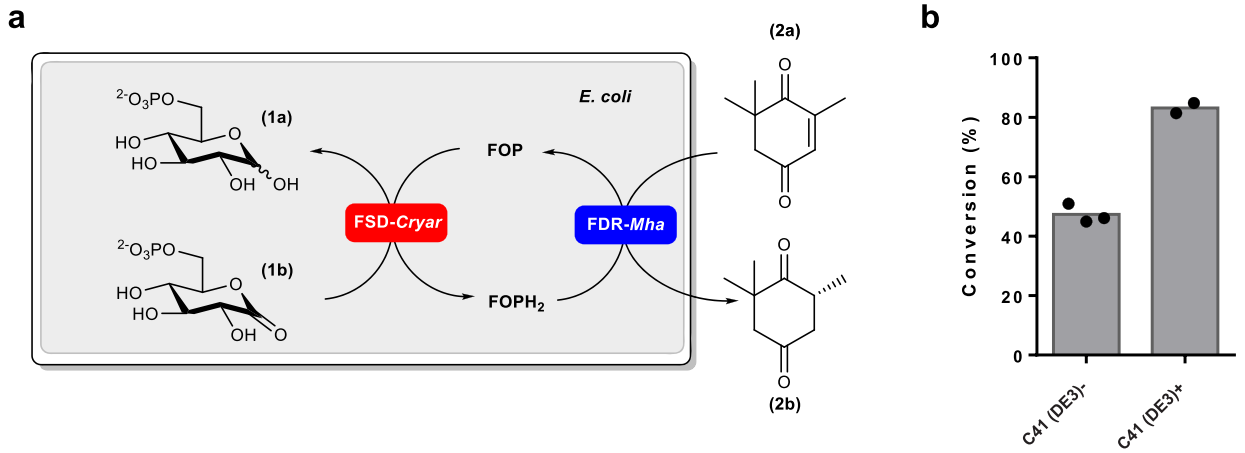

Figure 7. (a) Scheme of whole-cell FOP-mediated conversion of 2,2,6-trimethyl-2-cyclohexen-1,4-dione (**2a**). The in vivo synthesized FOP is reduced by FSD-Cryar, using glucose-6-phosphate (**1a**) as sacrificial electron source. FDR-Mha catalyzes the reduction of **2a** by $FOPH_2$. (b) Whole-cell conversion of ketoisophorone by *E. coli* C41 (DE3). C41 (DE3)−, wild-type strain. C41 (DE3)+, cells harboring pETDuet_*Ms*FbiC, pCDFDuet_*Sp*RFK E123L, and pCOLA_FSD/FDR.

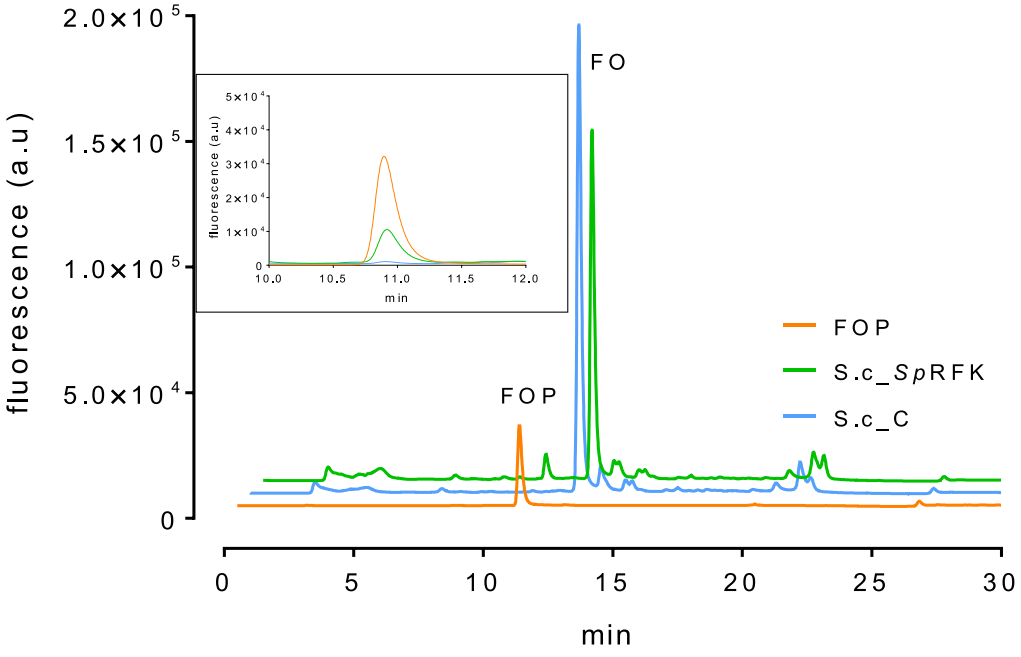

Figure 8. In vivo FOP production of *S. cerevisiae* expressing wild-type *Sp*RFK. The cell-free extract of *S. cerevisiae* expressing *Sp*RFK (green line) shows a peak corresponding to FOP which aligns with the purified FOP standard (orange line). The control strain without *Sp*RFK shows no measurable in vivo FOP formation (blue line). The inset shows a zoomed-in chromatogram area of FOP peaks.

E123L and grown at 37 °C in TB medium. For this estimation we used the following experimentally verified parameters: 1 $OD_{600} \triangleq 7.8 \times 10^8$ cells mL^{-1} and the *E. coli* cell volume is 4.4×10^{-15} L.[21,22] This intercellular FOP concentration is high enough to fuel several F_{420}-dependent enzymes.[15] Therefore, we attempted to do a whole-cell FOP-mediated conversion of ketoisophorone (2,6,6-trimethyl-2-cyclohexene-1,4-dione), using the deazaflavoenzymes sugar-6-phosphate dehydrogenase from *Cryptosporangium arvum* (FSD-*Cryar*) and the ene-reductase from *Mycobacterium hassiacum* (FDR-*Mha*) (Figure 7a).[23,29] Both genes were cloned into pCOLADuet-1 (Table S2) and coexpressed with pETDuet_*Ms*FbiC and pCDFDuet_*Sp*RFK E123L in C41 (DE3). After growing cells in TB medium, they were transferred to M9 medium with 1% glycerol and 7.5 mM ketoisophorone. After incubating the cells overnight, samples were taken for analysis. Reverse-phase HPLC showed that ketoisophorone was converted by both cultures of C41 (DE3) with and without the three plasmids. Yet, C41 (DE3) cells that contained the plasmid system converted significantly more ketoisophorone (83% compared to 47%) (Figure 7b). GC-MS was performed to verify the presence of the reductase product, 2,2,6-trimethylcyclohexane-1,4-dione, which was indeed present (Figure S5). Previous in vitro data on ketoisophorone reduction by FDR-Mha showed that the product had an e.e. of 72% (*S*).[23] Chiral GC of whole-cell conversions, however, showed an e.e. of 42% (*R*) for both C41

https://doi.org/10.1021/acssynbio.1c00552
ACS Synth. Biol. 2022, 11, 938−952

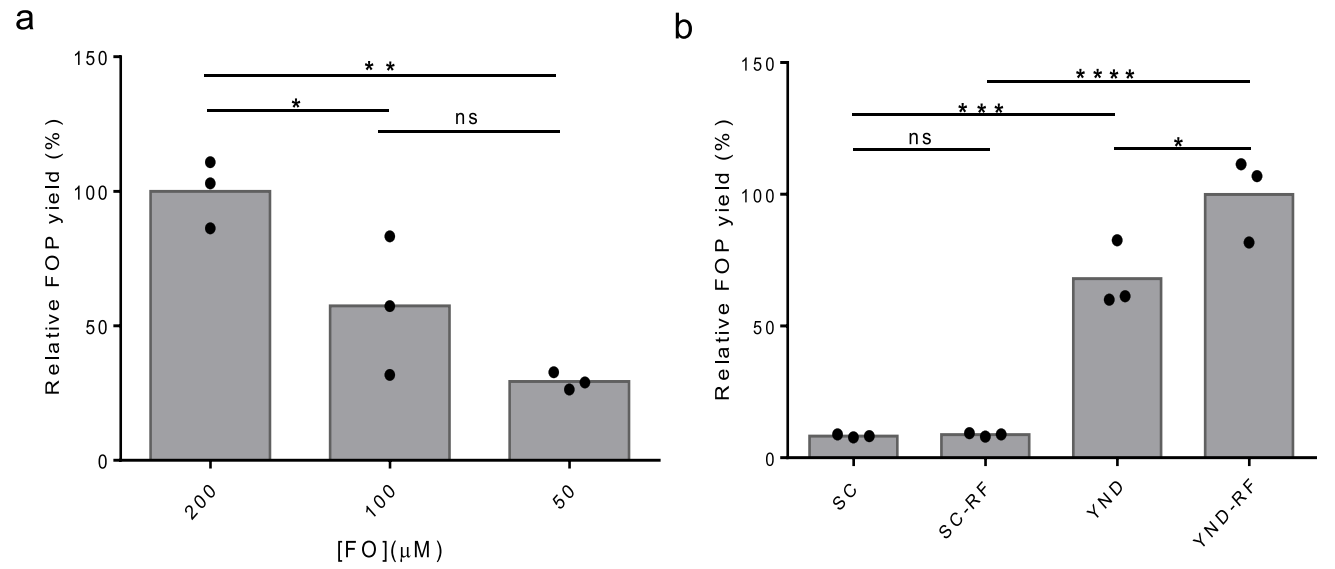

Figure 9. Media optimization for improving in vivo FOP conversion in *S. cerevisiae*. (a) Effect of FO concentration in media on FOP yield. (b) Effect of different media and riboflavin supplements. The dots show the individual data points of three independent samples and their averages are presented in bars. The average value of samples with highest FOP yield is set as 100% in both a and b. In all experiments the FOP yield was normalized by the cell density (OD_{600}) of the samples. The statistical significance of the data was analyzed by one-way ANOVA. ns, $p > 0.05$; *$p \leq 0.05$; **$p \leq 0.01$; ***$p \leq 0.001$.

(DE3) with and without the plasmid system (Figure S6). This is probably due to a racemization effect caused by endogenous *E. coli* reductases/dehydrogenases, as was also described previously by Dezavarei and Lee et al. for the whole-cell P450-mediated isophorene hydroxylation in *E. coli*.[30] Product racemization was also seen in crude extract of *Rhodococcus rhodochrous* ATCC 17895.[31]

In Vivo FOP Production by *Sp*RFK in *S. cerevisiae*. After confirming that *Sp*RFK converts FO to FOP, we tested the expression of the enzyme in *S. cerevisiae* for possible in vivo FOP formation in yeast. SDS-PAGE analysis revealed the soluble expression of *Sp*RFK in *S. cerevisiae* (Figure S7). The use of different promoters (pTEF1 and pPGK1) did not show any significant differences in the expression level and we continued further work with the pTEF1 promoter. Next, we tested whether the enzyme can produce a detectable amount of FOP in vivo. After growth of the yeast cells expressing *Sp*RFK in the medium supplemented with FO, the cell extracts were analyzed by HPLC. After 24 h of cultivation in the medium supplemented with FO, the cells containing wild-type *Sp*RFK showed FOP production with a yield of 0.24 ± 0.04 nmol per g dry biomass whereas wild-type cells lacking *Sp*RFK did not show any detectable amount of FOP (Figure 8). This result indicates that *Sp*RFK performs in vivo FO phosphorylation and that the native *S. cerevisiae* riboflavin kinase does not contribute to the FOP production. However, the yield was poor and would not be sufficient for FOP-dependent bioconversion. Therefore, further engineering and optimization is required for increasing the FOP yield and in vivo concentration.

For de novo biosynthesis of FOP, we attempted expression of several codon-optimized FO synthases in *S. cerevisiae*. However, functional expression of several FO synthases (FbiC from *M. smegmatis*, *Mycobacterium tuberculosis*, and *Chlamydomonas reinhardtii* and CofG/H from *M. jannaschii*) in *S. cerevisiae* failed (data not shown). Therefore, we focused on improving the in vivo FOP production using the chemically synthesized FO.

Effect of Media and FO Concentration on FOP Production. In addition to the catalytic performance of *Sp*RFK, indirect factors such as the growth condition of *S. cerevisiae* can also influence the in vivo FOP conversion. In order to optimize the condition for FOP production, we tested several variables and analyzed the FOP yield. The concentration of FO in the media may influence the in vivo FO concentration and cellular metabolism, which likely affects the final FOP yield. Three different FO concentrations (50, 100, and 200 μM) in the media were tested and showed a significant influence on the final FOP yield. While no apparent influence of FO on the growth of *S. cerevisiae* was observed, increasing FO concentration positively correlated with the final FOP yield (Figure 9a). The improvement of FOP yield is possibly due to an increase in intracellular FO concentration. Although it is possible that the uptake efficiency did not reach its maximum within the tested FO concentration range, we continued further experiments using 200 μM FO due to its poor solubility.

Next, we tested the influence of the media composition on the FOP yield. In general, for yeast cultivation, we used a synthetic defined medium (SC) which contains yeast nitrogen base (YNB), amino acids and vitamin supplements as well as 2% glucose. Except for the auxotrophic amino acids (Trp, His, Leu) for the yeast strain used (CEN. PK2−1C), all other supplemented amino acids are not essential for cell growth. To evaluate the effect of the supplements on FOP yield, we compared the FOP yield of wild-type *Sp*RFK containing cells grown on SC medium and YND (YNB + 2% glucose) medium supplemented only with the auxotrophic amino acids. The use of YND medium resulted in a more than 8-fold higher FOP yield compared to the use of SC medium (Figure 9b). During cultivation, no apparent effect on growth was observed and similar OD_{600} was measured (~5.6) upon harvesting after 24 h. This result indicates that the additional amino acids supplemented in SC medium negatively influence the in vivo FOP conversion. SDS-PAGE analysis (Figure S7) showed that the two different media did not significantly affect the *Sp*RFK expression level.

In *S. cerevisiae*, riboflavin is known to be transported through simple diffusion and/or the riboflavin transporter MCH5 whose

https://doi.org/10.1021/acssynbio.1c00552
ACS Synth. Biol. 2022, 11, 938−952

expression is up-regulated by low intracellular riboflavin concentration.[32] Due to the structural similarity, FO and riboflavin are likely transported by the same means and may affect the transportation efficiency of each other. We tested whether the absence of riboflavin would improve the FO uptake, thus increasing the FOP conversion, by measuring the FOP yield in both SC and YND medium lacking riboflavin. While using SC medium with and without riboflavin yielded similar amounts of FOP, cells grown in YND medium without riboflavin showed a 1.5 higher FOP yield compared to cells grown in YND medium (Figure 9b). Therefore, the effect of the riboflavin in media for FOP conversion seems to be dependent on the type of media. Whether the increased FOP yield is indeed due to improved transport is yet to be verified, as the current method used for FOP isolation and measurement does not distinguish between the intracellular FO and the FO which remain bound on the cell surfaces after washing steps. Therefore, we do not exclude the possibility of riboflavin affecting FOP conversion through other mechanisms, for example ones related to metabolism. In conclusion, among the conditions we tested, the use of YND medium with 200 μM FO lacking riboflavin seems to provide the best FOP yield.

In Vivo FOP Production Using *Sp*RFK E123L in *S. cerevisiae*. As *Sp*RFK variant E123L showed improved FOP production in *E. coli*, we expressed this mutant *Sp*RFK in *S. cerevisiae* and measured the FOP production level after the growth in FO containing medium. Unlike the significant increase of FOP production by the variant in *E. coli*, the yeast cells carrying the *Sp*RFK E123L did not show any improvement in FOP production. The mutant *Sp*RFK carrying cells produced similar or slightly lower amount of FOP compared to the cells expressing the wild-type *Sp*RFK. In fact, SDS-PAGE analysis shows (Figure S7) that the expression level of *Sp*RFK E123L is poor compared to the wild-type enzyme. The lower expression level of the mutant may cancel out the effect of its improved catalytic properties, hence resulting in unaffected in vivo FOP production levels. In order to discover an improved variant relevant for in vivo applications in yeast, we generated an in silico designed *Sp*RFK mutant library and performed screening based on the in vivo FOP production level.

SpRFK Library Construction and Screening. To improve the in vivo FOP production of *S. cerevisiae* by improving the catalytic properties of *Sp*RFK, we designed a structure-guided rational mutant library. We envisioned that modifying the residues that interact with the moieties that distinguish FO from riboflavin could improve binding of FO (Figure 10) as well as reduce the binding of riboflavin which could be an inhibitor for in vivo FOP production. Based on Rosetta CoupledMoves calculations[26] for FOP binding and visual inspection of the structure, we selected 6 residues (Thr45, Val64, Val79, Ser81, Glu123, and Leu132) for the combinatorial mutagenesis library. Each residue was subjected to the substitutions to one, two or three different amino acid residues (Table 1). In order to limit the library size in view of the screening capacity, the library was divided into two sublibraries based on the locations of the residues in relation to the substrate. By combining gene fragments containing mutations at the respective residues, using the Golden Gate assembly method, we obtained all the desired variants including two wild-type constructs.

The screening results revealed five variants (D1, D3, D4, D7, and E1, Figure 11) which improved in vivo FOP production in *S. cerevisiae*. Interestingly, a common mutation in these five variants is E123M and the best variant among them is the single

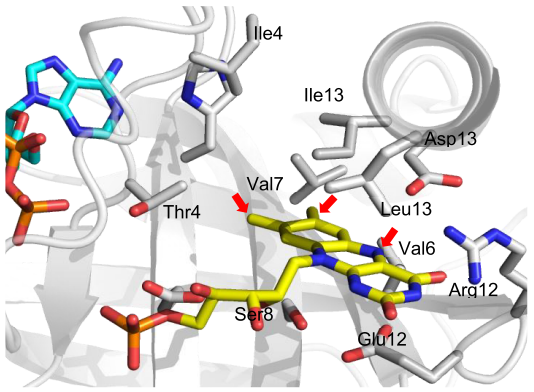

Figure 10. Substrate binding site structure of *Sp*RFK (1N07).[24] The residues surrounding the bound FMN (yellow) are shown in gray sticks and the residues that were subjected to be mutated during the in silico calculation are indicated with the residue numbers. The red arrows indicate the structural difference of FMN compared with FOP. A bound ADP molecule is shown in cyan sticks.

mutant E123M showing an over 3-fold increase in FOP production compared to the wild type. This indicates that the mutation E123M is beneficial for the in vivo FOP production in *S. cerevisiae* and that additional mutations decrease the positive effect of E123M. Therefore, we carried out further experiments using the E123M mutant kinase.

In order to verify the improvement of the selected variant on in vivo FOP production, we measured the FOP yield of cells expressing *Sp*RFK-E123M in bigger culture volumes and compared that to the wild type. Eight biological replicates of each wild type and the mutant containing cells were grown in YND medium lacking riboflavin, supplemented with 200 μM FOP for 24 h. The cell densities of all cultures at harvest were similar ranging from OD_{600} 5.2 to 6. On average, *Sp*RFK-E123M carrying cells produced 2.5-fold more FOP with the measured yield of 5.2 ± 0.9 nmol/gDCW compared to the wild type kinase carrying cells which produced 2.1 ± 0.2 nmol/gDCW. This translates to the accumulated intracellular FOP concentration of ~2 and ~0.8 μM, respectively, estimated based on the reported cell volume to biomass conversion.[33]

Steady-State Kinetics of *Sp*RFK Variants. Through the in vivo FOP production measurement we showed that the *Sp*RFK variants E123L and E123M increase FOP yield when expressed in *E. coli* and *S. cerevisiae*, respectively. Interpreted from the SDS-PAGE analyses, the improvements did not seem to be related with expression levels. Therefore, we measured the kinetic parameters of the purified enzymes in order to understand the factors that contributed to the improvements (Table 2). The variant E123L showed a slightly higher k_{cat} and half the K_M compared to the wild type, resulting in a 2.5-fold higher catalytic efficiency. The mutation E123M improved the catalytic properties on FO even further with a 2.5-fold higher k_{cat} and almost 3-fold lower K_M (7-fold higher catalytic efficiency compared to the wild type). The improved catalytic properties of both mutants explain the improved in vivo FOP yields. The lower K_M values for FO may especially be beneficial for low in vivo FO concentrations. Furthermore, the data suggest that the modestly improved catalytic property of the variant *Sp*RFK-E123L was sufficient to improve the FOP yield significantly in *E. coli* while it could not compensate its lowered expression in *S. cerevisiae*. Mutant E123L also seems to be slightly less inhibited by FMN than wild type and mutant E123M in vitro,

https://doi.org/10.1021/acssynbio.1c00552
ACS Synth. Biol. 2022, 11, 938−952

Table 1. *Sp*RFK Mutant Library Scheme

	library 1				library 2		
residues	Val64	Ser81	Glu123	Leu132	Thr45	Val79	Leu132
substitutions	I	A, V, C	L, M	I, M	D, E	M, L	I, M, E

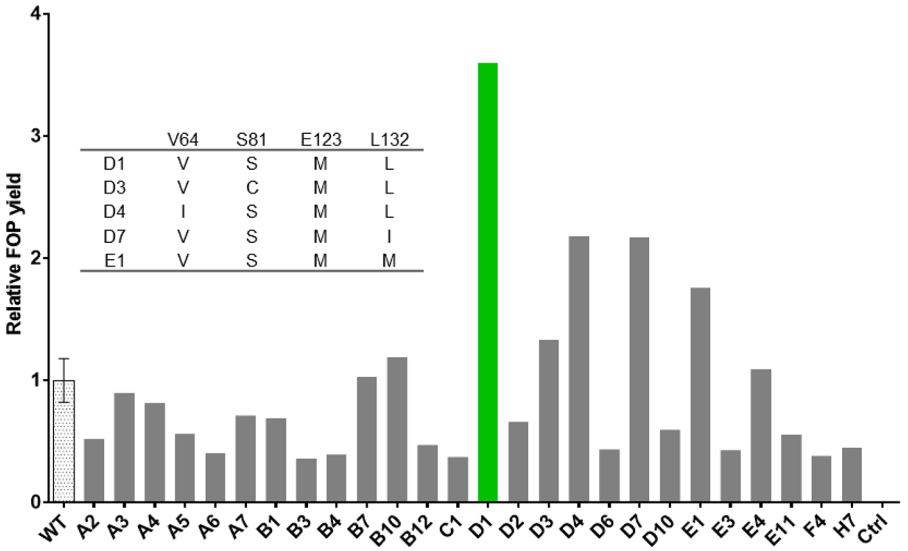

Figure 11. *Sp*RFK library screening result. The bars show the relative in vivo FOP yield of *S. cerevisiae* expressing the *Sp*RFK variants. Only the variants with measurable FOP production are shown. The mutations of all variants can be found in Table S3. The values of the single measurements of each sample were compared to the average value of three independent wild-type samples. The control sample (Ctrl) is *S. cerevisiae* cells without *Sp*RFK expression. The FOP yield is normalized by the cell density (OD_{600}). The inlet shows the best five variants.

Table 2. Kinetic Parameters of *Sp*RFK Variants[a]

	k_{cat} (s^{-1})	K_M (μM)	k_{cat}/K_M ($s^{-1}\cdot M^{-1}$)
*Sp*RFK	0.06 ± 0.006	100 ± 13	600
*Sp*RFK-E123L	0.08 ± 0.003	51 ± 3	1570
*Sp*RFK-E123M	0.15 ± 0.007	35 ± 3	4290

[a]All measurements were done at 30 °C, pH 7.0 (50 mM KPi). The k_{cat} values and the K_M values for FO are the average of duplicate measurements and the margins represent the standard deviations.

shown by less significant decrease in FO conversion in the presence of FMN, which could also contribute to the increase seen in the in vivo FOP yield in *E. coli* (see Table S4).

DISCUSSION

F_{420} is a naturally occurring deazaflavin redox cofactor found in archaea and Actinobacteria. Its very low redox potential and strict hydride transfer chemistry make it an interesting target for biocatalytic applications. Unfortunately, the low availability of this cofactor prevents it from being used for upscaled biotechnological applications thus far. In previous work we showed that a truncated version of F_{420}, the chemoenzymatically synthesized FO-5′-phosphate (FOP), could be used as an alternative cofactor for F_{420}-dependent enzymes.[15] FOP showed similar activities as F_{420} for enzymes from different structural classes, namely the F_{420}:NADPH oxidoreductase from *Thermobifida fusca* (Rossmann fold),[34] the sugar-6-phosphate dehydrogenase from *C. arvum* (TIM barrel)[29] and the ene-reductase from *M. hassiacum* (β-roll/split β-barel).[23] The low solubility of chemically synthesized FO, the relatively high cost and bulk availability of ATP and the instability of the kinase from *C. ammoniagenes*[35] prompted a search for alternative green synthesis routes for FOP. Whole-cell synthesis of FOP, either by supplying chemically synthesized FO in the media or by de novo biosynthesis, could be a scalable, environmentally friendly, and cheap way to synthesize this valuable cofactor for large-scale applications.

We pursued in vivo FOP synthesis by using either a FO synthase or chemically synthesized FO and a monofunctional riboflavin kinase from *S. pombe*, both in *E. coli* and *S. cerevisiae*. The amino acid sequences of the truncated *Ca*RFK and the *Sp*RFK share only 24% identity. The riboflavin binding site residues of these enzymes show quite some diversification as well. Whereas the *Ca*RFK required engineering for FOP conversion, wild-type *Sp*RFK already accepted FO as a substrate, showing an even higher FOP conversion yield compared to the mutant *Ca*RFK. Interestingly, amino acids at two residues near 7- and 8-methyl group of riboflavin in *Sp*RFK, Val79 and His98, correspond to the mutations that were previously made in *Ca*RFK for FO conversion. Although few riboflavin kinases were reported to convert various riboflavin analogues including 5-deazariboflavin, *Sp*RFK is the first riboflavin kinase to be reported to accept FO as a substrate without engineering.[35,36]

Using a FO synthase from *M. smegmatis* and *Sp*RFK variant E123L, we showed that FOP can be produced in vivo by *E. coli* C41 (DE3). The yield was 1.24 μmol L^{-1}, which is 45 times higher than the F_{420} yield of *E. coli* expressing the heterologous F_{420} biosynthesis pathway.[13] The simple two-step biosynthesis pathway of FOP, compared to the multistep synthesis of the more complex cofactor F_{420}, could be a possible reason for this observed difference. Recently, Shah et al. showed that the F_{420} yield in *E. coli* can be increased up to 2.33 μmol L^{-1} by varying carbon sources, which demonstrates the potential for improving non-natural cofactor production by using simple methods.[14] The FOP yield presented here closely resembles the F_{420} yield

https://doi.org/10.1021/acssynbio.1c00552
ACS Synth. Biol. 2022, 11, 938−952

Table 3. F_{420}/FOP Yields of Several F_{420} Producing Organisms and the *E. coli* FOP Producing System, as Presented in This Work

organism/strain	yield		growth time	cell yield (g/L)	potential hazards
	μmol/g	μmol/L			
M. smegmatis[10]	0.3	1.43	2−4 days	4.8	wound infection
Methanobacterium thermoautotrophicum[10]	1.7	0.85	3−5 days	0.5	flammable/explosive gas
Streptomyces flocculus[10]	0.62	4.43	3−4 days	7.2	toxic metabolites
E. coli BL21 (DE3)-F420[13]	–	0.027			–
E. coli C41 (DE3)-FOP	0.3	1.24	16 h	3.1	–

from *M. smegmatis*, which is 1.43 μmol L^{-1}. The estimated FOP productivity per unit of time (0.078 μmol L^{-1} h^{-1}), however, is much higher than that of F_{420} by *M. smegmatis*. *E. coli*—with doubling times as low as 20 min—grows much faster than *M. smegmatis*, with doubling times of 3 to 4 h. Therefore, expression strains of *E. coli* can be harvested already after 12 to 16 h, whereas *M. smegmatis* and other F_{420} production strains take 2−4 days (Table 3).

Another advantage of *E. coli* is the wealth of readily available genetic tools, which could be used to engineer genetically stable FOP production strains, and even whole-cell factories for FOP-mediated conversions. In this work we could indeed show—as a proof of concept—that whole-cell conversions could be performed by expressing the FOP biosynthesis machinery on two separate plasmids, as well as two additional enzymes for FOP reduction and compound conversion on a third plasmid. Although *E. coli* C41 (DE3) has a background reduction activity toward the employed substrate, we could show a significant increase in ketoisophorone conversions when the three plasmids were introduced, albeit with loss of the previously established (*S*)-selectivity in vitro.[23] Endogenous ketoisophorone reductions by native enzymes, producing racemic mixtures were also observed in previous studies.[30,31] In fact, the *E. coli* genome contains several homologues of YqjM, the NAD(P)-dependent ene reductase from *Bacillus subtilis*, capable of reducing ketoisophorone with (*R*)-enantioselectivity.[37−39] Identification and subsequent gene knock outs of the responsible enzymes could overcome this observed "racemization" problem provided that these enzymes are nonessential.[40] Further engineering could result in cell factories for efficient FOP-fueled enantioselective reductions that only require substrate, *E. coli* cells, and cheap growth media. The intracellular FOP concentration of up to 40 μM is high enough to support catalysis.[15] Also of great importance is the safety of *E. coli*, as compared to natural F_{420} sources, which might be opportunistic pathogens, may produce toxic waste products or need flammable, explosive gases for their growth (Table 3).

In addition to developing the FOP-producing *E. coli* strain, we also explored FOP production in *S. cerevisiae*, a representative eukaryotic microorganism. Besides the well-developed genetic and strain engineering tools, the advantage of using the yeast strain also lies on the easy implementation in industrial settings due to its robustness and harmless nature.[41] To the extent of our knowledge, in vivo production of F_{420} or other deazaflavins in yeast have not been reported so far. In a recent study, use of chemically synthesized FO for tetracycline biosynthesis in *S. cerevisiae* was demonstrated.[42] Although FO can be used for some F_{420}-dependent conversion, in vivo FOP production can expand the reaction scope owing to the phosphate group offering better binding to more F_{420}-dependent enzymes and less leakage from the cell. In this study, we show that it is possible to produce FOP in *S. cerevisiae* using the heterologously expressed *Sp*RFK and FO supplemented in the media.

In view of finding a variant for improved in vivo FOP conversion in *S. cerevisiae*, some 90 mutants were designed and screened for improved in vivo FOP yield. The screening results revealed 5 improved variants of which E123M showed the highest FOP yield. As also shown with the mutant E123L which improved in vivo FOP production in *E. coli*, residue Glu123 seems to play an important role for the activity toward FO. This residue in *Sp*RFK interacts with N5 of riboflavin, possibly stabilizing the substrate in the correct orientation.[24] We initially anticipated that replacing this residue with a hydrophobic amino acid would improve the in vivo FOP production of the enzyme by reduced inhibition by FMN as well as improving the activity toward FO. However, in vitro conversion assays measured in the presence of different FMN concentrations showed that both wild type and the variants are significantly inhibited by FMN (Table S4). Albeit that E123L shows slight less inhibition than wild type and E123M, which might have contributed to the improved FOP yield in *E. coli*.

Even though *Sp*RFK E123L showed a significant improvement in FOP production in *E. coli*, it did not increase the FOP yield in *S. cerevisiae* due to the lower expression level compared to wild-type *Sp*RFK. This result showed that the protein expression level can change due to a single mutation and that change is dependent on the host organism. It also indicates that improved in vitro steady state kinetic properties do not always result in better in vivo performance, especially when the improvement is modest as in the case of E123L.

Besides the enzyme engineering approach, we also optimized other aspects related to growth condition for improving the final FOP yield in *S. cerevisiae*. Through testing different media, we first discovered that using the minimal medium (YND) yields much higher (∼8-fold) FOP than using medium with amino acid supplements (SC). Essentially, SC medium is a YND medium with supplementary amino acids. There was no apparent effect of the media on growth behavior and the mechanism of the improved FOP conversion is unclear. The availability of extra amino acids in the media may affect the intracellular environment or metabolic flux in such a way that it influences the FOP production. For example, supplementing glycine, a precursor in purine synthesis, could increase the riboflavin synthesis, which could potentially prevent the FOP formation as more *Sp*RFK would be occupied with riboflavin rather than FO.[43,44] This result shows that sometimes less supplemented media are more beneficial for whole cell-based production. A previous study on FO production in *E. coli* also showed that using minimal media supplemented only with tyrosine, a FO precursor, gives higher FO yield than using a more completed media.[17]

Although *S. cerevisiae* is a riboflavin-prototroph and does not require additional riboflavin for growth,[45−47] it is included in generally used media. Omitting riboflavin from the media improved the FOP production in *S. cerevisiae*, which is anticipated to be the effect of less competition in uptake of

https://doi.org/10.1021/acssynbio.1c00552
ACS Synth. Biol. 2022, 11, 938−952

FO. However, further studies on how riboflavin affects FO uptake or in vivo FOP formation is required. The higher FOP yield caused by increased FO concentration (up to 200 μM) in the media also indirectly indicates a suboptimal FO transport to the cell, although the result may as well be related with high K_M of wild-type *Sp*RFK for FO. Overall, the best condition found in this study for FOP production in *S. cerevisiae* is to use YND medium lacking riboflavin supplemented with 200 μM FO. Using this condition and the best *Sp*RFK variant discovered from the library, E123M, we increased the FOP yield by over 20-fold compared to the unoptimized condition using SC medium and the wild-type *Sp*RFK. However, the final improved yield (5.2 ± 0.9 nmol/gCDW) is still very modest. With further improvement by strain and enzyme engineering as well as optimization of growth conditions, FOP-producing *S. cerevisiae* can potentially be used for interesting bioconversion applications.

CONCLUSION

In this study, we showed that it is possible to produce the artificial deazaflavin cofactor FOP in both *E. coli* and *S. cerevisiae*. In *E. coli*, de novo FOP biosynthesis was achieved by heterologous expression of a FO synthase from *M. smegmatis* and a riboflavin kinase from *S. pombe*. The improved FOP yield obtained through optimization was sufficient to demonstrate a whole-cell conversion with a F_{420}-dependent reductase. The FOP yield in *E. coli* is very similar to the F_{420} yield in *M. smegmatis*, which is regarded as the best strain for F_{420}-production. The initially very low in vivo FOP yield in *S. cerevisiae* was also significantly improved through enzyme engineering and media optimization. In conclusion, our findings presented here may further the development of deazaflavin-dependent whole-cell conversions in both bacteria and yeast strains. Using these strains for the safe, easy to use, scalable, and cost-effective FOP synthesis might also boost deazaflavin mediated in vitro (bio)catalysis.

ASSOCIATED CONTENT

Supporting Information

The Supporting Information is available free of charge at https://pubs.acs.org/doi/10.1021/acssynbio.1c00552.

List of codon optimized genes and vector constructs that were used in this study, with their codon optimized sequences; SDS-PAGE gels and the results of FO conversion experiments in the presence of FMN (PDF)

AUTHOR INFORMATION

Corresponding Author

Marco W. Fraaije − *Molecular Enzymology Group, University of Groningen, 9747AG Groningen, The Netherlands;* orcid.org/0000-0001-6346-5014; Email: m.w.fraaije@rug.nl

Authors

Misun Lee − *Molecular Enzymology Group, University of Groningen, 9747AG Groningen, The Netherlands*

Jeroen Drenth − *Molecular Enzymology Group, University of Groningen, 9747AG Groningen, The Netherlands*

Milos Trajkovic − *Molecular Enzymology Group, University of Groningen, 9747AG Groningen, The Netherlands*

René M. de Jong − *DSM Biotechnology Center, 2613 AX Delft, The Netherlands*

Complete contact information is available at: https://pubs.acs.org/10.1021/acssynbio.1c00552

Author Contributions

M.L., J.D., and M.W.F. designed the project. J.D. designed and performed the experiments and analyzed the results for in vivo FOP production in *E. coli*. M.L. designed and performed the experiments and analyzed the results for in vivo FOP production in *S. cerevisiae*. R.M.d.J. designed the in silico RFK mutants, and M.T. synthesized FO and assisted in chemical analyses. M.L. performed mutagenesis on RFK gene and steady-state kinetic analysis on engineered RFK variants. M.L., J.D., and M.W.F. wrote the manuscript.

Author Contributions

[§]M.L. and J.D. contributed equally.

Funding

The research is financially supported by Dutch research council NWO (NWO-VICI-Fraaije and NWO-LIFT-YeastPlus grants), Royal DSM, and Syngenta.

Notes

R.d.J. is affiliated with DSM, a global company active in Nutrition, Health and Sustainable Living.

ACKNOWLEDGMENTS

We also thank Marcus Hans, Cees Sagt, and Alrik Los from Royal DSM, as well as Jason Vincent and Matthew Bennett from Syngenta for valuable scientific discussions.

REFERENCES

(1) Sheldon, R. A.; Brady, D.; Bode, M. L. The Hitchhiker's Guide to Biocatalysis: Recent Advances in the Use of Enzymes in Organic Synthesis. *Chem. Sci.* **2020**, *11*, 2587−2605.

(2) Shah, M. V.; Antoney, J.; Kang, S. W.; Warden, A. C.; Hartley, C. J.; Nazem-Bokaee, H.; Jackson, C. J.; Scott, C. Cofactor F_{420}-Dependent Enzymes: An Under-Explored Resource for Asymmetric Redox Biocatalysis. *Catalysts* **2019**, *9*, 868.

(3) Taylor, M.; Scott, C.; Grogan, G. F_{420}-Dependent Enzymes - Potential for Applications in Biotechnology. *Trends Biotechnol.* **2013**, *31*, 63−64.

(4) Walsh, C. Naturally Occurring 5-Deazaflavin Coenzymes: Biological Redox Roles. *Acc. Chem. Res.* **1986**, *19*, 216−221.

(5) Lowe, H. J.; Clark, W. M. Studies on Oxidation-Reduction. XXIV. Oxidation-Reduction Potentials of Flavin Adenine Dinucleotide. *J. Biol. Chem.* **1956**, *221*, 983−992.

(6) Draper, R. D.; Ingraham, L. L. A Potentiometric Study of the Flavin Semiquinone Equilibrium. *Arch. Biochem. Biophys.* **1968**, *125*, 802−808.

(7) Hemmerich, P.; Massey, V. Flavin and 5-Deazaflavin: A Chemical Evaluation of 'Modified' Flavoproteins with Respect to the Mechanisms of Redox Biocatalysis. *FEBS Lett.* **1977**, *84*, 5−21.

(8) Jacobson, F.; Walsh, C. Properties of 7,8-Didemethyl-8-Hydroxy-5-Deazaflavins Relevant to Redox Coenzyme Function in Methanogen Metabolism. *Biochemistry* **1984**, *23*, 979−988.

(9) Grinter, R.; Greening, C. Cofactor F_{420}: An Expanded View of Its Distribution, Biosynthesis and Roles in Bacteria and Archaea. *FEMS Microbiol. Rev.* **2021**, *45*, 1−46.

(10) Isabelle, D.; Simpson, D. R.; Daniels, L. Large-Scale Production of Coenzyme F_{420}-5,6 by Using *Mycobacterium Smegmatis*. *Appl. Environ. Microbiol.* **2002**, *68*, 5750−5755.

(11) Bashiri, G.; Rehan, A. M.; Greenwood, D. R.; Dickson, J. M. J.; Baker, E. N. Metabolic Engineering of Cofactor F_{420} Production in *Mycobacterium Smegmatis*. *PLoS One* **2010**, *5*, e15803.

(12) Braga, D.; Last, D.; Hasan, M.; Guo, H.; Leichnitz, D.; Uzum, Z.; Richter, I.; Schalk, F.; Beemelmanns, C.; Hertweck, C.; Lackner, G. Metabolic Pathway Rerouting in *Paraburkholderia Rhizoxinica* Evolved

Long-Overlooked Derivatives of Coenzyme F_{420}. *ACS Chem. Biol.* **2019**, *14*, 2088−2094.
(13) Bashiri, G.; Antoney, J.; Jirgis, E. N. M.; Shah, M. V.; Ney, B.; Copp, J.; Stuteley, S. M.; Sreebhavan, S.; Palmer, B.; Middleditch, M.; Tokuriki, N.; Greening, C.; Scott, C.; Baker, E. N.; Jackson, C. J. A Revised Biosynthetic Pathway for the Cofactor F_{420} in Prokaryotes. *Nat. Commun.* **2019**, *10*, 1−12.
(14) Shah, M. V.; Nazem-Bokaee, H.; Antoney, J.; Kang, S. W.; Jackson, C. J.; Scott, C. Improved Production of the Non-Native Cofactor F_{420} in *Escherichia Coli*. *Sci. Rep.* **2021**, *11*, 21774.
(15) Drenth, J.; Trajkovic, M.; Fraaije, M. W. Chemoenzymatic Synthesis of an Unnatural Deazaflavin Cofactor That Can Fuel F_{420}-Dependent Enzymes. *ACS Catal.* **2019**, *9*, 6435.
(16) Choi, K. P.; Kendrick, N.; Daniels, L. Demonstration That FbiC Is Required by *Mycobacterium Bovis* BCG for Coenzyme F_{420} and FO Biosynthesis. *J. Bacteriol.* **2002**, *184*, 2420−2428.
(17) Graham, D. E.; Xu, H.; White, R. H. Identification of the 7,8-Didemethyl-8-Hydroxy-5-Deazariboflavin Synthase Required for Coenzyme F_{420} Biosynthesis. *Arch. Microbiol.* **2003**, *180*, 455−464.
(18) Decamps, L.; Philmus, B.; Benjdia, A.; White, R.; Begley, T. P.; Berteau, O. Biosynthesis of F_0, Precursor of the F_{420} Cofactor, Requires a Unique Two Radical-SAM Domain Enzyme and Tyrosine as Substrate. *J. Am. Chem. Soc.* **2012**, *134*, 18173−18176.
(19) Engler, C.; Kandzia, R.; Marillonnet, S. A One Pot, One Step, Precision Cloning Method with High Throughput Capability. *PLoS One* **2008**, *3*, e3647.
(20) Lee, M. E.; DeLoache, W. C.; Cervantes, B.; Dueber, J. E. A Highly Characterized Yeast Toolkit for Modular, Multipart Assembly. *ACS Synth. Biol.* **2015**, *4*, 975−986.
(21) Volkmer, B.; Heinemann, M. Condition-Dependent Cell Volume and Concentration of *Escherichia Coli* to Facilitate Data Conversion for Systems Biology Modeling. *PLoS One* **2011**, *6*, e23126.
(22) Myers, J. A.; Curtis, B. S.; Curtis, W. R. Improving Accuracy of Cell and Chromophore Concentration Measurements Using Optical Density. *BMC Biophys.* **2013**, *6*, 4.
(23) Mathew, S.; Trajkovic, M.; Kumar, H.; Nguyen, Q. T.; Fraaije, M. W. Enantio- and Regioselective *Ene*-Reductions Using $F_{420}H_2$-Dependent Enzymes. *Chem. Commun.* **2018**, *54*, 11208−11211.
(24) Bauer, S.; Kemter, K.; Bacher, A.; Huber, R.; Fischer, M.; Steinbacher, S. Crystal Structure of *Schizosaccharomyces Pombe* Riboflavin Kinase Reveals a Novel ATP and Riboflavin-Binding Fold. *J. Mol. Biol.* **2003**, *326*, 1463−1473.
(25) Leman, J. K.; Weitzner, B. D.; Lewis, S. M.; Adolf-Bryfogle, J.; Alam, N.; Alford, R. F.; Aprahamian, M.; Baker, D.; Barlow, K. A.; Barth, P.; Basanta, B.; Bender, B. J.; Blacklock, K.; Bonet, J.; Boyken, S. E.; Bradley, P.; Bystroff, C.; Conway, P.; Cooper, S.; Correia, B. E.; Coventry, B.; Das, R.; De Jong, R. M.; DiMaio, F.; Dsilva, L.; Dunbrack, R.; Ford, A. S.; Frenz, B.; Fu, D. Y.; Geniesse, C.; Goldschmidt, L.; Gowthaman, R.; Gray, J. J.; Gront, D.; Guffy, S.; Horowitz, S.; Huang, P. S.; Huber, T.; Jacobs, T. M.; Jeliazkov, J. R.; Johnson, D. K.; Kappel, K.; Karanicolas, J.; Khakzad, H.; Khar, K. R.; Khare, S. D.; Khatib, F.; Khramushin, A.; King, I. C.; Kleffner, R.; Koepnick, B.; Kortemme, T.; Kuenze, G.; Kuhlman, B.; Kuroda, D.; Labonte, J. W.; Lai, J. K.; Lapidoth, G.; Leaver-Fay, A.; Lindert, S.; Linsky, T.; London, N.; Lubin, J. H.; Lyskov, S.; Maguire, J.; Malmström, L.; Marcos, E.; Marcu, O.; Marze, N. A.; Meiler, J.; Moretti, R.; Mulligan, V. K.; Nerli, S.; Norn, C.; Ó'Conchúir, S.; Ollikainen, N.; Ovchinnikov, S.; Pacella, M. S.; Pan, X.; Park, H.; Pavlovicz, R. E.; Pethe, M.; Pierce, B. G.; Pilla, K. B.; Raveh, B.; Renfrew, P. D.; Burman, S. S. R.; Rubenstein, A.; Sauer, M. F.; Scheck, A.; Schief, W.; Schueler-Furman, O.; Sedan, Y.; Sevy, A. M.; Sgourakis, N. G.; Shi, L.; Siegel, J. B.; Silva, D. A.; Smith, S.; Song, Y.; Stein, A.; Szegedy, M.; Teets, F. D.; Thyme, S. B.; Wang, R. Y. R.; Watkins, A.; Zimmerman, L.; Bonneau, R. Macromolecular Modeling and Design in Rosetta: Recent Methods and Frameworks. *Nat. Methods* **2020**, *17*, 665−680.
(26) Ollikainen, N.; de Jong, R. M.; Kortemme, T. Coupling Protein Side-Chain and Backbone Flexibility Improves the Re-Design of Protein-Ligand Specificity. *PLoS Comput. Biol.* **2015**, *11*, e1004335.
(27) Gietz, R. D.; Schiestl, R. H. High-Efficiency Yeast Transformation Using the LiAc/SS Carrier DNA/PEG Method. *Nat. Protoc.* **2007**, *2*, 31−34.
(28) Herguedas, B.; Lans, I.; Sebastián, M.; Hermoso, J. A.; Martínez-Júlvez, M.; Medina, M. Structural Insights into the Synthesis of FMN in Prokaryotic Organisms. *Acta Crystallogr. Sect. D Biol. Crystallogr.* **2015**, *71*, 2526−2542.
(29) Mascotti, M. L.; Kumar, H.; Nguyen, Q. T.; Ayub, M. J.; Fraaije, M. W. Reconstructing the Evolutionary History of F_{420}-Dependent Dehydrogenases. *Sci. Rep.* **2018**, *8*, 17571.
(30) Dezvarei, S.; Lee, J. H. Z.; Bell, S. G. Stereoselective Hydroxylation of Isophorone by Variants of the Cytochromes P450 CYP102A1 and CYP101A1. *Enzyme Microb. Technol.* **2018**, *111*, 29−37.
(31) Chen, B. S.; Médici, R.; van der Helm, M. P.; van Zwet, Y.; Gjonaj, L.; van der Geest, R.; Otten, L. G.; Hanefeld, U. *Rhodococcus* Strains as Source for Ene-Reductase Activity. *Appl. Microbiol. Biotechnol.* **2018**, *102*, 5545−5556.
(32) Reihl, P.; Stolz, J. The Monocarboxylate Transporter Homolog Mch5p Catalyzes Riboflavin (Vitamin B2) Uptake in *Saccharomyces Cerevisiae*. *J. Biol. Chem.* **2005**, *280*, 39809−39817.
(33) Klis, F. M.; de Koster, C. G.; Brul, S. Cell Wall-Related Bionumbers and Bioestimates of *Saccharomyces Cerevisiae* and *Candida Albicans*. *Eukaryot. Cell* **2014**, *13*, 2−9.
(34) Kumar, H.; Nguyen, Q. T.; Binda, C.; Mattevi, A.; Fraaije, M. W. Isolation and Characterization of a Thermostable F_{420}:NADPH Oxidoreductase from *Thermobifida Fusca*. *J. Biol. Chem.* **2017**, *292*, 10123−10130.
(35) Iamurri, S. M.; Daugherty, A. B.; Edmondson, D. E.; Lutz, S. Truncated FAD Synthetase for Direct Biocatalytic Conversion of Riboflavin and Analogs to Their Corresponding Flavin Mononucleotides. *Protein Eng. Des. Sel.* **2013**, *26*, 791−795.
(36) Kearney, E. B. The Interaction of Yeast Flavokinase with Riboflavin Analogues. *J. Biol. Chem.* **1952**, *194*, 747−754.
(37) Brewster, R. C.; Suitor, J. T.; Bennett, A. W.; Wallace, S. Transition Metal-Free Reduction of Activated Alkenes Using a Living Microorganism. *Angew. Chemie - Int. Ed.* **2019**, *58*, 12409−12414.
(38) Miura, K.; Tomioka, Y.; Suzuki, H.; Yonezawa, M.; Hishinuma, T.; Mizugaki, M. Molecular Cloning of the *NemA* Gene Encoding *N*-Ethylmaleimide Reductase from *Escherichia Coli*. *Biol. Pharm. Bull.* **1997**, *20*, 110−112.
(39) Winkler, C. K.; Tasnádi, G.; Clay, D.; Hall, M.; Faber, K. Asymmetric Bioreduction of Activated Alkenes to Industrially Relevant Optically Active Compounds. *J. Biotechnol.* **2012**, *162*, 381−389.
(40) Fitzpatrick, T. B.; Amrhein, N.; Macheroux, P. Characterization of YqjM, an Old Yellow Enzyme Homolog from *Bacillus Subtilis* Involved in the Oxidative Stress Response. *J. Biol. Chem.* **2003**, *278*, 19891−19897.
(41) Parapouli, M.; Vasileiadi, A.; Afendra, A.-S.; Hatziloukas, E. *Saccharomyces Cerevisiae* and Its Industrial Applications. *AIMS Microbiol.* **2020**, *6*, 1−31.
(42) Herbst, E.; Lee, A.; Tang, Y.; Snyder, S. A.; Cornish, V. W. Heterologous Catalysis of the Final Steps of Tetracycline Biosynthesis by *Saccharomyces Cerevisiae*. *ACS Chem. Biol.* **2021**, *16*, 1425.
(43) Liu, S.; Hu, W.; Wang, Z.; Chen, T. Production of Riboflavin and Related Cofactors by Biotechnological Processes. *Microb. Cell Fact.* **2020**, *19*, 1−16.
(44) Schlüpen, C.; Santos, M. A.; Weber, U.; De Graaf, A.; Revuelta, J. L.; Stahmann, K. P. Disruption of the SHM2 Gene, Encoding One of Two Serine Hydroxymethyltransferase Isoenzymes, Reduces the Flux from Glycine to Serine in *Ashbya Gossypii*. *Biochem. J.* **2003**, *369*, 263−273.
(45) Santos, M. A.; Garcia-Ramirez, J. J.; Revuelta, J. L. Riboflavin Biosynthesis in *Saccharomyces Cerevisiae*. Cloning, Characterization, and Expression of the RIB5 Gene Encoding Riboflavin Synthase. *J. Biol. Chem.* **1995**, *270*, 437−444.
(46) Abbas, C. A.; Sibirny, A. A. Genetic Control of Biosynthesis and Transport of Riboflavin and Flavin Nucleotides and Construction of

https://doi.org/10.1021/acssynbio.1c00552
ACS Synth. Biol. 2022, 11, 938−952

Robust Biotechnological Producers. *Microbiol. Mol. Biol. Rev.* **2011**, *75*, 321−360.
(47) Gudipati, V.; Koch, K.; Lienhart, W. D.; Macheroux, P. The Flavoproteome of the Yeast *Saccharomyces Cerevisiae*. *Biochim. Biophys. Acta - Proteins Proteomics* **2014**, *1844*, 535−544.

https://doi.org/10.1021/acssynbio.1c00552
ACS Synth. Biol. 2022, 11, 938−952